Accepted Manuscript

Effect of sustained loading and environmental conditions on the creep behavior of an epoxy adhesive for concrete structures strengthened with CFRP laminates

M. Emara, L. Torres, M. Baena, C. Barris, M. Moawad

PII: S1359-8368(17)31764-X

DOI: 10.1016/j.compositesb.2017.07.026

Reference: JCOMB 5162

To appear in: *Composites Part B*

Received Date: 24 May 2017

Revised Date: 10 July 2017

Accepted Date: 25 July 2017

Please cite this article as: Emara M, Torres L, Baena M, Barris C, Moawad M, Effect of sustained loading and environmental conditions on the creep behavior of an epoxy adhesive for concrete structures strengthened with CFRP laminates, *Composites Part B* (2017), doi: 10.1016/ j.compositesb.2017.07.026.

Effect of sustained loading and environmental conditions on the creep behavior of an epoxy adhesive for concrete structures strengthened with CFRP laminates

M. Emara[a,b,*], L. Torres[a], M. Baena[a], C. Barris[a], M. Moawad[a,b]

[a] *AMADE, Polytechnic School, Universitat de Girona, Campus Montilivi s/n, 17071 Girona, Spain.*
[b] *Structural Engineering Dept., Faculty of Engineering, Zagazig University, B.O. Box 44519, Zagazig, Sharkia, Egypt.*

Abstract

In this paper,the creep behavior of a structural epoxy adhesive used for strengthening Reinforced Concrete (RC) structures with Carbon Fiber Reinforced Polymer (CFRP) laminates is studied through an experimental program. Long-term tensile creep tests were carried out inside a climate chamber using sustained loading levels, temperature and humidity as the parameters for the study. The specimens were kept loaded inside the climate chamber for 1000 hours. Standard Tensile Tests (STT), Dynamic Mechanical Analysis (DMA) and Differential Scanning Calorimetry (DSC) tests were carried out to characterize the adhesive used. In general, the results obtained revealed that changing temperature and humidity conditions greatly affect not only instantaneous and creep strain values, but also time to failure, leading to a change in the overall behavior of the adhesive.

Keywords: A. Thermosetting resin; B. Creep; D. Mechanical testing; Sustained loading.

*Corresponding author. Tel: +34 627114755
Email addresses: mohamed.emara@udg.edu (M. Emara), lluis.torres@udg.edu (L. Torres), marta.baena@udg.edu (M. Baena), cristina.barris@udg.edu (C. Barris), mohamed.moawad@udg.edu (M. Moawad)

1. Introduction

Fiber Reinforced Polymers (FRPs) are now widely used in civil engineering and construction. FRP materials are successfully being applied as an alternative to conventional steel, either as reinforcing or for strengthening Reinforced Concrete (RC) structures. The most common procedures for strengthening RC structures are Externally Bonded (EB) and Near Surface Mounted (NSM): these techniques use different FRP products [1], of which Carbon FRP (CFRP) laminates are one of the most widely employed. For both methodologies to be efficient, good bonding conditions are normally required to control the composite action that develops between the FRP reinforcement and the concrete [2, 3]. For NSM strengthening technique, the most common and best-performing groove filler is, because of its excellent mechanical properties, a two-component epoxy [4]. Epoxy adhesives are used as the load-bearing material connecting FRP reinforcement to concrete because they have several advantages such as the capacity to transfer stresses along the bonded length without the loss of structural integrity, or the ability of minimize stress concentration by redistributing stresses more uniformly [5].

Previous studies [4, 6–11] showed that the mechanical properties of adhesive materials greatly affect bond behavior, as well as load-bearing, failure capacities and the failure mode, not only for the strengthening system, but also for many other applications such as composite beams [12–14].

The long-term performance of a strengthened structure under a sustained load, of prime importance for different safety aspects in design, is mainly dependent on the performance of the materials which make up the strengthening system. The viscoelastic behavior of epoxy adhesives under the effect of a sustained load may affect bond and load carrying capacity over time and cause deformations as well as redistribute stresses [15–17].

The creep behavior of epoxy adhesives is stress-dependent. In the linear viscoelastic

region, creep strain is a linear function of stress, which means creep compliance is independent of the stress levels applied. As the stress level increases, the behavior normally deviates from linear to nonlinear [18]. Experimental results presented in [16] show that the creep behavior of epoxy resins is dependent on the sustained stress level applied. Results obtained showed that increasing the percentage of the applied sustained stress, from 15% to 30% of the ultimate stress, increased the creep coefficient from 1 to 2.87 after 100 days of loading. Costa and Barros [19] registered considerable creep deformations (where creep strain increased by up to 180% of the instantaneous strain) in epoxy adhesive specimens subjected to different sustained levels of stress (20%, 40% and 60% of the tensile strength) under constant environmental conditions of 20 °C temperature and 60% relative humidity. The results obtained revealed that for up to 60% of the sustained load level, the epoxy resin used could be considered a linear viscoelastic/viscoplastic material. Results presented in [20] show that a linear viscoelastic behavior was observed up to a sustained stress level of 40% of the ultimate stress. In this study, tensile creep tests on an epoxy adhesive were performed at 20 °C with 55% relative humidity and two levels of sustained stress equal to 30% and 40% of the ultimate stress were applied. The strains obtained after 80 days, at 40% of sustained stress, increased by 140% compared with the initial strain at loading. Majda and Skrodzewicz [21] carried out creep tests on an epoxy adhesive using four levels of sustained load (33%, 43%, 54%, and 65% of the tensile strength) as specimens were subjected to ambient conditions. The results obtained showed that the adhesive used exhibited a nonlinear viscoelastic behavior over the range of the stress levels applied in the investigation.

Environmental conditions may significantly affect the mechanical behavior adhesives. Findings from the study reported in [22] show that when the temperature was increased from 22 °C to 100 °C there was a 20%-37% reduction in the modulus of elasticity of the adhesive being tested. In the same study, when the temperature applied was higher than its corresponding glass transition temperature (T_g), a 98% reduction in the modulus

of elasticity of the adhesive was observed, thus emphasizing that the tensile modulus and strength of the epoxy resin can drop drastically when temperature approaches the adhesive's T_g. Another study reported in [23] showed that both the tensile stiffness and strength of the adhesive being tested decreased from 14.1 GPa and 45.0 MPa at 35 °C to 0.16 GPa and 5.27 MPa at 60 °C, respectively. These results suggest that the viscoelastic responses of materials essentially become highly nonlinear when the temperature is close to T_g and that the service temperature of epoxy adhesives should be strictly limited by this transition temperature.

Humidity is also considered to be an influencing parameter, as the epoxy-based adhesives are vulnerable to moisture, especially in extremely humid environments [18]. Exposure to high levels of humidity can cause plasticization effects and chemical modifications in the epoxy resin [24, 25], as well as a considerable decrease in T_g.

From the analysis of the literature it is seen that, although a number of studies focused on the creep behavior of epoxy adhesives have been carried out, there is still a need to further investigate the influence parameters likely to greatly affect their performance might have on them. Among these parameters, sustained load level, temperature and humidity appear to be those that have a determinant influence. This paper presents the results of an experimental program to investigate the tensile creep behavior of a structural epoxy adhesive being used in CFRP RC strengthening systems. The main parameters included in the study are sustained load level, temperature and humidity.

2. Experimental program

The experimental program was composed of both short-term and long-term tensile tests. Standard Tensile Tests (STT), Dynamic Mechanical Analysis (DMA) and Differential Scanning Calorimetry (DSC) tests were carried out to characterize the adhesive used. Tensile creep tests were performed to investigate the creep behavior of the adhesive under varying temperatures and humidity levels.

2.1. Epoxy adhesive characterization

S&P Resin 220, which is usually used for bonding Carbon Fiber Reinforced Polymer (CFRP) laminates, is the commercially produced solvent-free, thixotropic two component epoxy resin adhesive used in this study. According to the manufacturer [26], the package contained component A (a light gray-colored resin) and component B (a black colored hardener). Component A contains (5%-10%) Neopentyl glycol diglycidyl ether and (20%-25%) Bisphenol A, while component B has (1%-2.5%) Piperazine, (20%-25%) Triethylenetetramine, (3.6%) Diazaoctanethylenediamin and (20%-25%) Poly (oxypropylene) diamine. Both components should be mixed slowly, in a proportion of 4A:1B (in weight), until a uniformly gray color (without any streaks) is obtained.

2.1.1. Scanning Electron Microscope (SEM)

To check the porosity and chemical composition of the epoxy resin after curing, specimen surfaces were viewed using a Scanning Electron Microscope (SEM). The observation was carried out using the Backscattered Electron (BSE) technique.

2.1.2. Standard Tensile Test (STT)

To determine the tensile strength and modulus of elasticity of the adhesive, dog-bone shaped specimens were prepared in accordance with ISO 527-2 [27] (see Figure 1), and STTs were carried out following the ISO 527-1 specifications [28]. After casting, specimens were left to cure for 10 days in laboratory conditions (20 °C and 55% relative humidity). Each specimen was instrumented with two longitudinal strain gauges glued onto the center of each face. The width and thickness of the specimens tested were measured at three different positions to determine their average cross section. Finally, the tensile tests were performed in a universal testing machine with displacement control at a loading rate of 1 mm/min (see Figure 2). Load and longitudinal strains were registered during the test and tensile stress-strain curves were obtained.

[Figure 1 about here.]

[Figure 2 about here.]

2.1.3. Differential Scanning Calorimetry (DSC)

DSC is one of the methods used to determine the T_g of materials. This technique provides quantitative and qualitative information about physical and chemical changes that involve either endothermic or exothermic processes, or changes in heat capacity. When the temperature reaches the glass transition zone, the material experiences a change in heat capacity and, by registering and measuring this change, the T_g can be obtained [29]. In this experimental program, isothermal DSC tests were carried out using the DSC Q2000. A heating rate of 10 °C/min was applied using nitrogen as the purge gas at 50 mL/min. The initial and final temperatures were 25 °C and 80 °C, respectively.

2.1.4. Dynamic Mechanical Analysis (DMA)

The DMA test is an alternative method to determining the T_g and viscoelastic properties of polymeric amorphous materials. This method is based on a frequency response analysis that uses a constant, non-destructive oscillatory strain (or stress) at selected frequencies and temperatures, while recording the resulting stress (or strain) response of the sample material. The METTLER TOLEDO DMA/SDTA861e analyzer with a 3-point bending test configuration and 45 mm between supports was used in this study (see Figure 3). The specimens were subjected to a heating rate of 2 °C/min within a temperature range of 30 °C to 100 °C. A 10 μm, constant displacement amplitude was applied at a frequency of 1 Hz. The glass transition temperature was studied by analyzing the storage modulus ($E^{'}$), the loss modulus ($E^{''}$) and the loss factor (tanδ) as functions of temperature (for further details see Section 3.2).

[Figure 3 about here.]

2.2. Tensile Creep Test

Dog-bone shaped specimens (like those shown in Figure 1) were used for the tensile creep tests. Tests were carried out in a climate chamber to ensure constant temperature and humidity. Once cast, specimens were left to cure in normal laboratory conditions (20 °C and 55% relative humidity) for 10 days. Once cured, they were conditioned inside the climate chamber under test conditions for three days before applying the loads. Loads were applied using gravity loading systems with a multiplication factor of 4 (see Figure 4). Each specimen was instrumented with two strain gauges glued onto the center of each face (see Figure 4(b). The strain gauges were connected to an automatic acquisition system to register the longitudinal strain during the test period (i.e. 1000 hours).

Details of test series are presented in Table 1. Each series corresponds to one combination of the environmental conditions. Furthermore, the three levels of sustained loading were applied in each series. In Table 1, the first column contains the name of the test series, while in the second column each of the specimens is identified by the letter S, followed by the sustained load level applied, the environmental conditions under which the test was carried out (C1, C2, C3 and C4) and the final letter identifies the two identical specimens. The third, fourth and fifth columns show the sustained loading levels applied as a percentage of the maximum tensile strength, the temperature, and the percentage of relative humidity, respectively. The temperature and relative humidity of the four environmental conditions were: 20 °C and 55% RH for C1, 20 °C and 90% RH for C2, 40 °C and 55% RH for C3 and 40 °C and 90% RH for C4. The sustained load levels applied were 20%, 40% and 60% of the tensile strength (i.e. 4 MPa, 8 MPa and 12 MPa, respectively), which are similar to those used in the literature [19–21] and are intended to cover the linear part of the short-term stress-strain behavior.

[Figure 4 about here.]

[Table 1 about here.]

3. Test results

3.1. Tensile mechanical properties

Stress-strain curves obtained from the STT showing an average maximum tensile stress of 20 MPa and an average failure strain of 3375 $\mu\epsilon$ are presented in Figure 5. The modulus of elasticity was calculated, in accordance with ISO 527-1 [28], as the slope of the secant line in the stress-strain diagram between 0.05% and 0.25% strains obtaining a value of 6600 MPa. Results obtained showed a coherence with the findings reported in [30], in which the same adhesive type was tested after three days of curing at 22 °C.

[Figure 5 about here.]

3.1.1. Scanning Electron Microscope (SEM) results

Results obtained from the SEM showed a high density and uniform distribution of mineral fillers (see Figure 6). Four main objects were identified and analyzed (see Table 2). A more in-depth analysis associated with the potentialities of SEM (Energy Dispersive X-Ray-EDX) allows for the position and combinations of elements to be identified, indicating the presence of barium sulphate (sulfur, barium), titanium dioxide (titanium, oxygen), epoxy matrix (carbon, oxygen) and quartz (silicon, oxygen).

[Figure 6 about here.]

[Table 2 about here.]

3.2. Glass transition temperature (T_g)

The two test methods (DSC and DMA) were used to determine the T_g of the adhesive used after 10 days of curing at 20 °C. Results from the DSC test are usually presented in terms of heat flow against temperature. To determine T_g, three temperatures were measured: (i) the extrapolated onset temperature T_{eig}, (ii) the mid-point temperature T_{mg} and (iii) the extrapolated end temperature T_{efg} (see inbox in Figure 7). According

to standards [29, 31], the T_{mg} temperature is more meaningful and may be designated as the T_g for most applications. Additionally, some specimens were left for curing during 1000 hours at 20 °C showing a T_g equal to 56.4 °C (obtained as the T_{mg} from DSC test) .

[Figure 7 about here.]

Values of T_g from DMA can be obtained by analyzing the evolution of the three different parameters provided by the test (see Figure 8). The storage modulus curve ($E^{'}$), represents the elastic part and provides the stiffness of the viscoelastic material, being proportional to the energy stored during a loading cycle. The loss modulus curve ($E^{''}$) is proportional to the energy dissipated during one loading cycle, and represents the viscous part. The loss factor (tanδ) curve, computed as the ratio of loss modulus to storage modulus, represents the relative contribution of the viscous vs. elastic properties, is a measure of the energy lost and is expressed in terms of the recoverable energy.

[Figure 8 about here.]

In this experimental program, T_g was calculated using three distinct methods: (i) the onset of the storage modulus curve drop, (ii) the peak value of loss modulus curves and (iii) the loss factor (tanδ) peak. T_g values obtained with both the DSC and DMA techniques are presented in Table 3, and show that T_g cannot be considered as a unique temperature, but rather it should be considered as a range of temperatures -as indicated elsewhere [32]. It should be mentioned that temperature transitions are more easily detected with DMA than with DSC [33], as mechanical changes are more dramatic than changes in heat capacity. DMA is able to detect short range motion before the glass transition range is attained and thus identify the onset of the main chain motion. Measurements on materials with low moisture contents may also present problems when tested by DSC because of indistinguishable transitions and limited accuracy [34], and this may be a reason different values of T_g are obtained with the DSC and DMA tests.

[Table 3 about here.]

3.3. Tensile creep test results

3.3.1. Instantaneous behavior

The initial instantaneous strains registered for the four series after applying the sustained load, (after the specimens had been conditioned), are presented in Figure 9. Regardless of the environmental conditions, increasing the sustained loading level caused an almost linear increase in the initial instantaneous strain. This can be observed in Figure 9, where the lines indicate the evolution of initial strains with respect to the sustained load level applied for each series. The average increase of instantaneous strain was 108% and 188% when the sustained load level changed from 20% to 40% and to 60%, respectively.

In all test series, the lowest change in the instantaneous strains due to changing the environmental conditions was observed at 20% of sustained loading . The increase in the instantaneous strain resulting from changing the humidity conditions from 55% to 90%, for both 20 °C and 40 °C, seemed to be very low (less than 6%), while the increase in temperature was larger (around 17% in average). Increase of both, temperature and humidity, had the largest effect (around 21%).

Additionally, it can be observed that, by increasing the sustained loading, the percentages of increase in the instantaneous initial strain were reasonably constant, with average increments of 3%, 16% and 21% for series 2, 3 and 4, respectively, when compared to series 1. Conditioning of the tested specimens prior to applying the sustained load allowed the environmental conditions to have an effect on the adhesive, showing that temperature seemed to have a greater effect than humidity did. It should be mentioned that at 40 °C the temperature was relatively close to the T_g of the resin (see Figures 7 and 8), which may be the reason for the higher variations.

[Figure 9 about here.]

3.3.2. Long-term behavior

Following ISO and ASTM standards [35, 36], the evolution of longitudinal strain with time was registered for each specimen for 1000 hours, thus enabling the creep strain and the creep compliance curves with time to be obtained. Creep compliances were calculated according to:

$$J_c(t) = \frac{\epsilon(t)}{\sigma_0} \tag{1}$$

where J_c(t) is the creep compliance at time (t), $\epsilon(t)$ and σ_o are the strain at time (t) and the applied sustained stress, respectively. On the other hand, creep coefficients were calculated as follows:

$$\phi(t) = \frac{\epsilon(t) - \epsilon(t_o)}{\epsilon(t_o)} \tag{2}$$

where $\phi(t)$is the creep coefficient at time (t), $\epsilon(t)$ and $\epsilon(t_o)$ are the strain at time (t) and the instantaneous strain, respectively. Values of creep compliance and coefficients for the different series, at the end of the testing period, are summarized in Table 4.

[Table 4 about here.]

Figure 10 shows the evolution of strain and creep compliance ($J_c(t)$) with time under environmental conditions of 20 °C and 55% RH and different levels of sustained loading (series 1). In this series, similar curves of creep compliance vs. time were obtained for all the sustained load levels applied. This can be evidence of the linear viscoelastic behavior of the specimens up to 60% of the sustained load, as the creep compliance is somewhat independent of the stress levels. The creep rate and creep strain values increased by increasing the sustained loading level. By the end of the test period, i.e. 1000 hours, specimens S40C1 and S60C1 showed creep coefficients 2.6% and 37%, respectively, higher than that of specimen S20C1. For this test series, the specimens lasted until the end of the test period without failure.

[Figure 10 about here.]

Figure 11 shows the evolution of strain and creep $J_c(t)$ with time under 20 °C and 90% relative humidity and different levels of sustained loading (series 2). The assumption of the linear viscoelastic behavior was shown to be valid for levels of sustained loading less than or equal to 40%, and similar creep compliance evolution with time was observed, whereas a loss of linearity in the viscoelastic behavior was observed when 60% of sustained load level was applied. In addition to the nonlinear viscoelastic behavior, an increase in the humidity caused premature failure after 60 hours in the specimen with a 60% of sustained loading (S60C2).

After 1000 hours of loading, the creep coefficient of specimen S40C2 was 4% higher than that of specimen S20C2. Compared to first test series, the creep coefficient increased by 27% and 29% for specimens under sustained load levels of 20% and 40%, respectively, and higher creep strain values were registered with time. In this test series, the application of a high level of humidity resulted in an increase in water absorption, leading to plasticization effects and chemical modifications of the epoxy resin as well as changes in its mechanical properties and the behavior [25, 37].

[Figure 11 about here.]

Figure 12 shows the evolution of strain and $J_c(t)$ with time under 40 °C and 55% relative humidity, and different levels of sustained loading (series 3). In this test series, different creep compliance evolutions were again observed depending on the level of sustained load applied, which means that this level of temperature significantly affected the linearity of the viscoelastic behavior of the adhesive. Applying 40 °C , which is near to glass transition range, resulted in rapid and dramatic changes in the stiffness and strength of the epoxy resin [20, 32], causing higher strain values and early failure due to creep rupture, as observed in specimens S40C3 and S60C3 which failed after 346 hours and 30 hours, respectively. The specimen loaded at 20% of the sustained load, i.e. S20C3, was the only one to last until the end of testing period, showing a high value of creep coefficient of 10.88. Compared to the first test series, the creep coefficient increased by 394%.

[Figure 12 about here.]

Figure 13 shows the evolution of strain and creep compliance ($J_c(t)$) with time under 40 °C and 90% relative humidity and the different levels of sustained loading (series 4). None of the specimens in this series lasted until the end of test and shorter failure times were observed: specimens S20C4, S40C4 and S60C4 failed at 113 hours, 1 hour and 0.5 hour, respectively. Higher creep strains, creep rates and creep compliance values were observed compared to the other test series. This behavior was expected, as specimens were subjected to a combined effect of an increase in both temperature and humidity. The exposure to a high level of humidity resulted in a decrease in T_g and a rapid degradation in the strength and the stiffness of the adhesive. In addition, simultaneously applying the high temperatures resulted in a greater degradation in the stiffness and strength as the resin started to enter the rubbery stage [22, 24].

[Figure 13 about here.]

Observing the results obtained in this experimental program, sustained loading levels, temperature and relative humidity were all found to have a significant effect on the tensile creep behavior of the adhesive studied.

4. Conclusions

An experimental program to study the tensile creep behavior of a commercially sold structural epoxy adhesive used in concrete strengthening with FRPs has been carried out. The program comprised four test series in which sustained stress levels, temperature and humidity were the main parameters studied. Based on the results obtained, the following conclusions can be drawn:

- The average increase of instantaneous strain, for all test series, was 108% and 188% when the sustained load level changed from 20% to 40% and to 60%, respectively.
- Increasing the humidity level to 90% at 20 °C did not significantly affect the instantaneous initial strain for a specific sustained load levels.
- Changing the environmental conditions (temperature from 20 °C to 40 °C and humidity from 55% to 90%) affected the instantaneous initial strain only in the cases of medium and high levels of sustained loading (i.e. 40% and 60%), while almost no effect was observed at low level of sustained loading (i.e. 20%).
- The linear viscoelastic behavior of the adhesive is present in up to 60% of sustained load under 20 °C and 55% RH. This limit starts to decrease when the environmental conditions are changed.
- Increasing the relative humidity, increases creep rates and creep coefficient. Increasing the humidity level up to 90% increases the creep coefficient by 27% and 29% in case of 20% and 40% of sustained load, respectively.

- At 90% humidity with normal temperature conditions, failure was observed after 60 hours of loading in the case of specimens with 60% of sustained loading.
- At 40 °C, very high creep coefficients and creep strains can be obtained and shorter times to failure are observed. The registered times were 346 hours and 30 hours at sustained load levels of 40% and 60%, respectively.
- Under the combined effect of high temperature (40 °C) and humidity (90%), no specimen lasted until the end of the test period and shorter times to failure were observed due to rapid degradation in the adhesive's strength and the stiffness. The registered times to failure were 113 hours, 1 hour and 0.5 hour at sustained load levels of 20%, 40% and 60%, respectively.
- High levels of temperature and humidity cause a rapid increase in the creep behavior.
- Temperature, compared to that of humidity, seemed to have a greater effect on the instantaneous initial strain, creep coefficient and time to failure.

Acknowledgement

The authors acknowledge the support provided by the Spanish Government (Ministerio de Economa y Competividad). Project Ref. BIA2013-46944-C2-2-P. The first author would like to acknowledge the support from the European Network for Durable Reinforcement and Rehabilitation Solutions (endure), a Marie Sklodowska Curie Initial Training Network (Contract number MC-ITN2013-607851).

References

[1] ACI-440.2.R . Guide for the Design and Construction of Externally Bonded FRP Systems for Strengthening Concrete Structures. ACI American Concrete Institute,Advancing concrete knowledge 2008;ACI Committee 440.

[2] De Lorenzis L, Nanni A. Bond between near-surface mounted fiber-reinforced polymer rods and concrete in structural strengthening. ACI structural Journal 2002;99(2):123–32.

[3] Coelho MR, Sena-Cruz JM, Neves LA. A review on the bond behavior of FRP NSM systems in concrete. Construction and Building Materials 2015;93:1157–69.

[4] De Lorenzis L, Teng J. Near-surface mounted FRP reinforcement: An emerging technique for strengthening structures. Composites Part B: Engineering 2007;38(2):119–43.

[5] Feng CW, Keong CW, Hsueh YP, Wang YY, Sue HJ. Modeling of long-term creep behavior of structural epoxy adhesives. International journal of adhesion and adhesives 2005;25(5):427–36.

[6] Borchert K, Zilch K, Knöfel R. Epoxy resin bonded NSM FRP reinforcement under environmental and load conditions. In: Structural Engineering Research Frontiers. ASCE; 2007, p. 1–12.

[7] Seracino R, Jones NM, Ali M, Page MW, Oehlers DJ. Bond strength of near-surface mounted FRP strip-to-concrete joints. Journal of Composites for Construction 2007;11(4):401–9.

[8] Borchert K, Zilch K. Bond behaviour of NSM FRP strips in service. Structural Concrete 2008;9(3):127–42.

[9] Rizzo A, De Lorenzis L. Behavior and capacity of RC beams strengthened in shear with NSM FRP reinforcement. Construction and Building Materials 2009;23(4):1555–67.

[10] Sharaky I, Torres L, Baena M, Miàs C. An experimental study of different factors

affecting the bond of NSM FRP bars in concrete. Composite Structures 2013;99:350–65.

[11] Torres L, Sharaky IA, Barris C, Baena M. Experimental study of the influence of adhesive properties and bond length on the bond behaviour of NSM FRP bars in concrete. Journal of Civil Engineering and Management 2016;22(6):808–17.

[12] Ascione F, Mancusi G, Spadea S, Lamberti M, Lebon F, Maurel-Pantel A. On the flexural behaviour of gfrp beams obtained by bonding simple panels: an experimental investigation. Composite Structures 2015;131:55–65.

[13] Lamberti M, Maurel-Pantel A, Ascione F, Lebon F. Influence of web/flange reinforcement on the gfrp bonded beams mechanical response: A comparison with experimental results and a numerical prediction. Composite Structures 2016;147:247–59.

[14] Ascione F, Feo L, Lamberti M, Penna R. Experimental and numerical evaluation of the axial stiffness of the adhesive connections in composite beams. Composite Structures 2017;176:702–14.

[15] Mazzotti C, Savoia M. Stress redistribution along the interface between concrete and FRP subject to long-term loading. Advances in Structural Engineering 2009;12(5):651–61.

[16] Meshgin P, Choi KK, Taha MMR. Experimental and analytical investigations of creep of epoxy adhesive at the concrete-FRP interfaces. International Journal of Adhesion and Adhesives 2009;29(1):56–66.

[17] Ferrier E, Michel L, Jurkiewiez B, Hamelin P. Creep behavior of adhesives used for external FRP strengthening of RC structures. Construction and Building Materials 2011;25(2):461–7.

[18] Feng CW. Prediction of long-term creep behavior of epoxy adhesives for structural applications. Master's thesis; Texas A&M University.; 2004.

[19] Costa I, Barros J. Tensile creep of a structural epoxy adhesive: Experimental and analytical characterization. International Journal of Adhesion and Adhesives 2015;59:115–24.

[20] Silva P, Valente T, Azenha M, Sena-Cruz J, Barros J. Viscoelastic response of an epoxy adhesive for construction since its early ages: Experiments and modelling. Composites Part B: Engineering 2016;In Press.

[21] Majda P, Skrodzewicz J. A modified creep model of epoxy adhesive at ambient temperature. International Journal of Adhesion and Adhesives 2009;29(4):396–404.

[22] Da Silva LF, Adams R. Measurement of the mechanical properties of structural adhesives in tension and shear over a wide range of temperatures. Journal of Adhesion Science and Technology 2005;19(2):109–41.

[23] Moussa O, Vassilopoulos AP, de Castro J, Keller T. Time–temperature dependence of thermomechanical recovery of cold-curing structural adhesives. International Journal of Adhesion and Adhesives 2012;35:94–101.

[24] De'Nève B, Shanahan M. Water absorption by an epoxy resin and its effect on the mechanical properties and infra-red spectra. Polymer 1993;34(24):5099–105.

[25] Lettieri M, Frigione M. Effects of humid environment on thermal and mechanical properties of a cold-curing structural epoxy adhesive. Construction and Building Materials 2012;30:753–60.

[26] S&P220 . 220 epoxy adhesive:Two-component epoxy resin-based adhesive for s&p FRP systems. 2013.

[27] ISO-527-2 . Plastics - Determination of tensile properties - Part 2: Test conditions for moulding and extrusion plastics. ISO International Organization for Standardization 2012;Geneva, Switzerland.

[28] ISO-527-2 . Plastics - Determination of tensile properties - Part 1: General principles. ISO International Organization for Standardization 2012;Geneva, Switzerland.

[29] ISO-11357-2 . Plastics - Differential Scanning Calorimetry - Part 2: Determination of glass transition temperature. ISO International Organization for Standardization 1999;Geneva, Switzerland.

[30] Michels J, Sena-Cruz J, Czaderski C, Motavalli M. Structural strengthening with prestressed cfrp strips with gradient anchorage. Journal of Composites for Construction 2013;17(5):651–61.

[31] ASTM-D3418 . Standard Test Methods of Polymers by Differential Scanning Calorimetry. ASTM International 1999;West Conshohocken, PA.

[32] Michels J, Widmann R, Czaderski C, Allahvirdizadeh R, Motavalli M. Glass transition evaluation of commercially available epoxy resins used for civil engineering applications. Composites Part B: Engineering 2015;77:484–93.

[33] Abiad MG, Campanella OH, Carvajal MT. Assessment of thermal transitions by dynamic mechanical analysis DSC using a novel disposable powder holder. Pharmaceutics 2010;2(2):78–90.

[34] Kalichevsky M, Jaroszkiewicz E, Ablett S, Blanshard J, Lillford P. The glass transition of amylopectin measured by DSC, DMTA and NMR. Carbohydrate Polymers 1992;18(2):77–88.

[35] ISO-899-1 . Plastics - Determination of creep behaviour - Part 1: Tensile creep. ISO International Organization for Standardization 2003;Geneva, Switzerland.

[36] ASTM-D2290 . Standard Test Methods for Tensile, Compressive, and Flexural Creep and Creep-Rupture of Plastics. ASTM American Society for Testing and Materials 2001;Pennsylvania, US.

[37] De Neve B, Shanahan M. Effects of humidity on an epoxy adhesive. International Journal of Adhesion and Adhesives 1992;12(3):191–6.

List of Figures

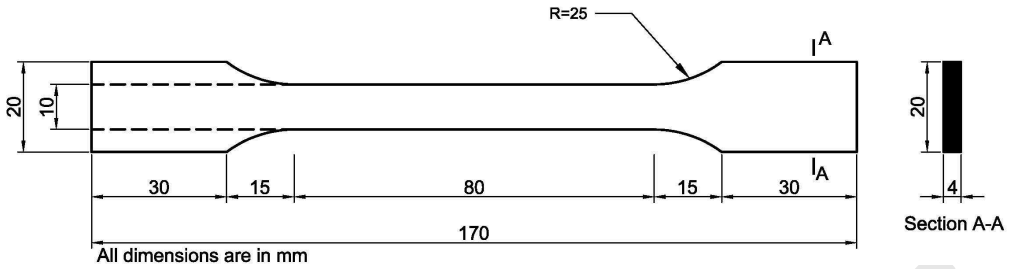

Figure 1: Test specimen dimensions

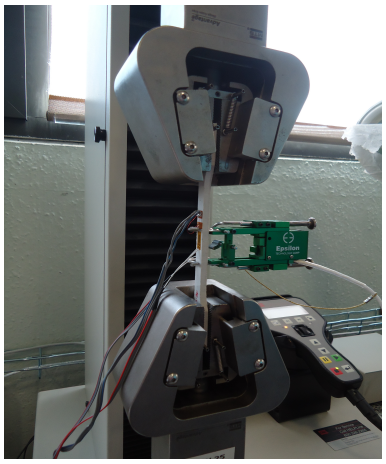

Figure 2: Tensile test setup and instrumentation

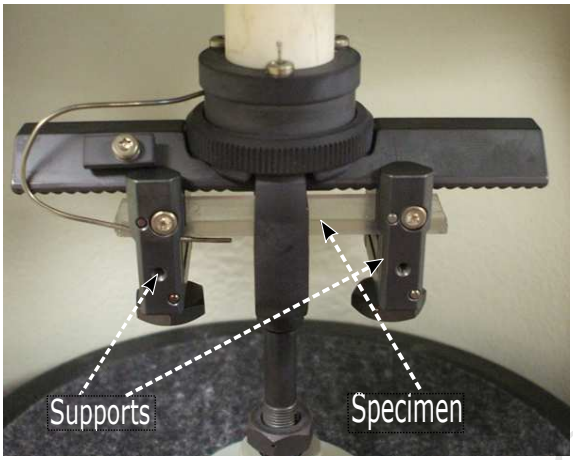

Figure 3: DMA test setup

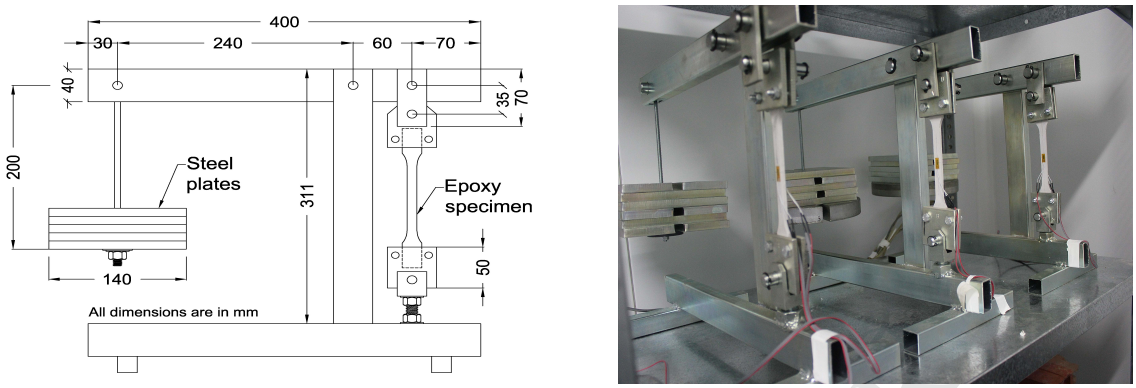

(a) (b)

Figure 4: Tensile creep test (a) Loading frame details and (b) Test setup and instrumentation.

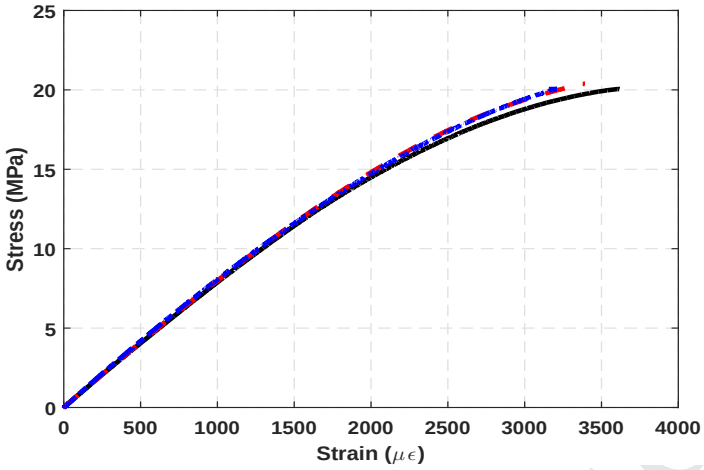

Figure 5: Stress vs. strain results (3 specimens)

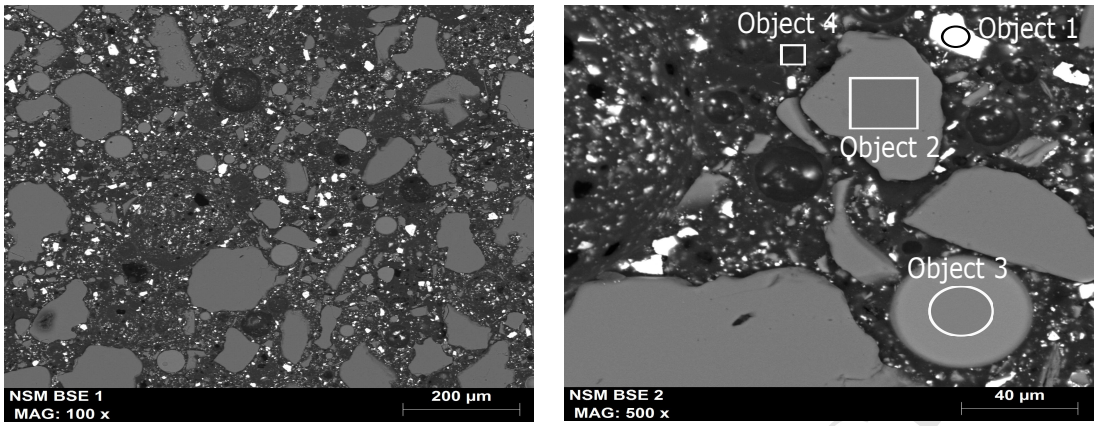

(a) (b)

Figure 6: SEM images (a) Particle distribution and (b) Chemical composition

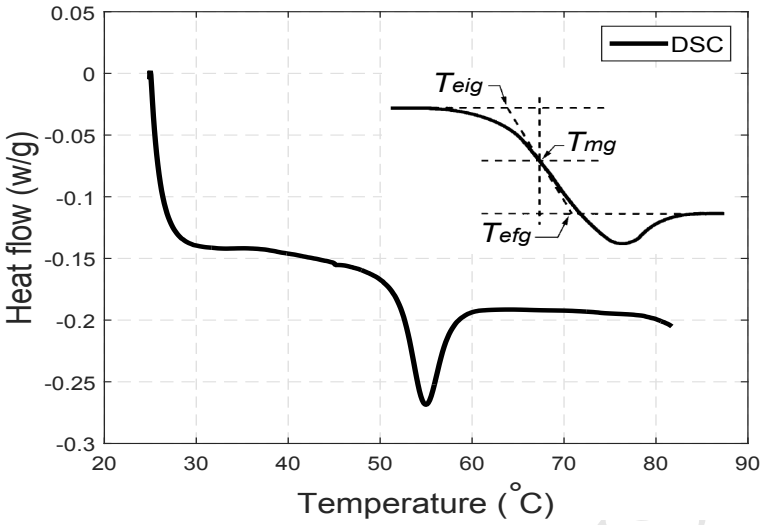

Figure 7: DSC test results

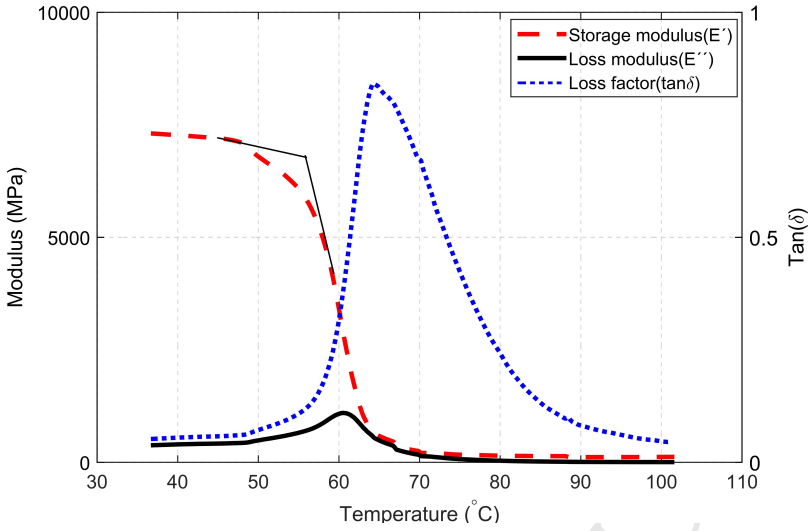

Figure 8: DMA test results

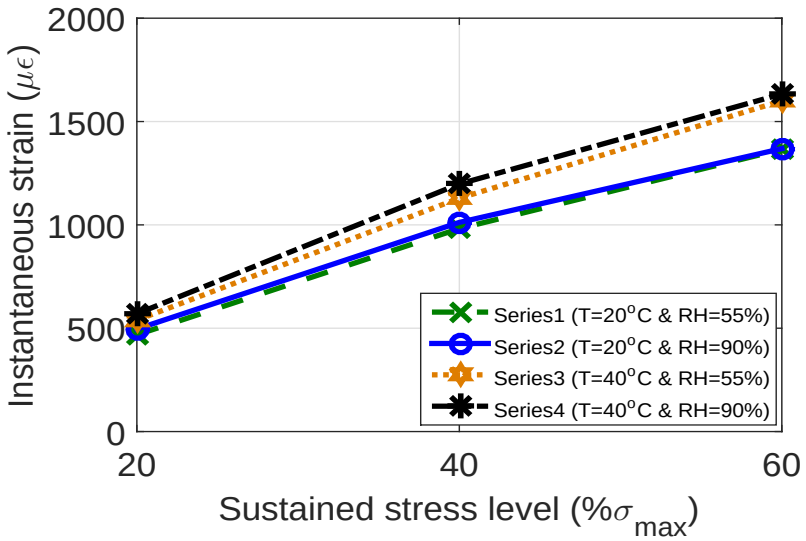

Figure 9: Instantaneous strain values

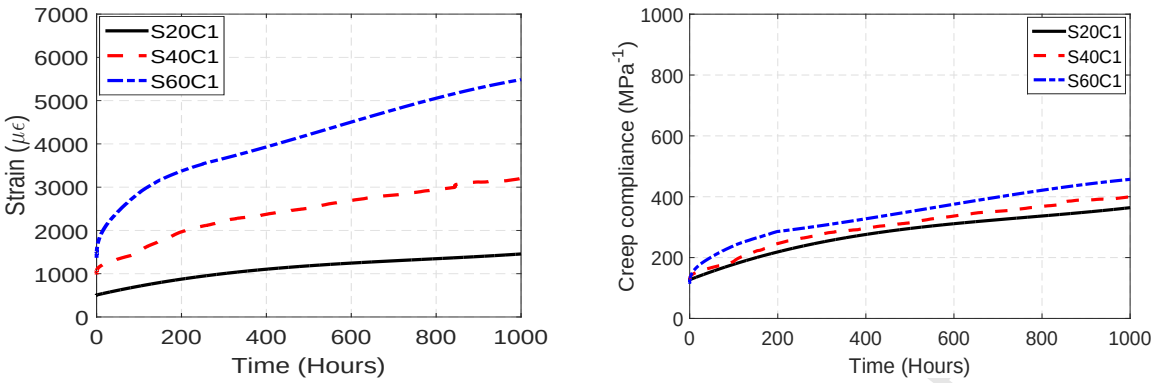

(a) (b)

Figure 10: Series 1 (a)Tensile strain with time and (b)Creep compliance with time

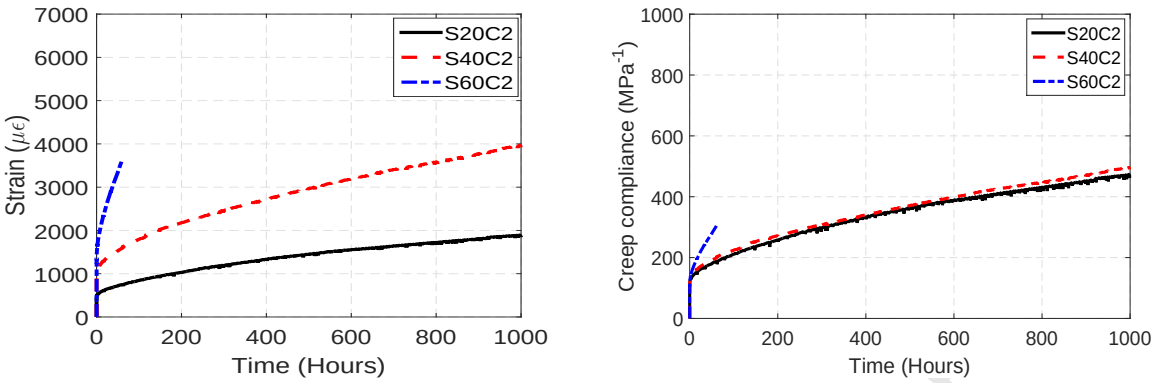

Figure 11: Series 2 (a)Tensile strain with time and (b)Creep compliance with time

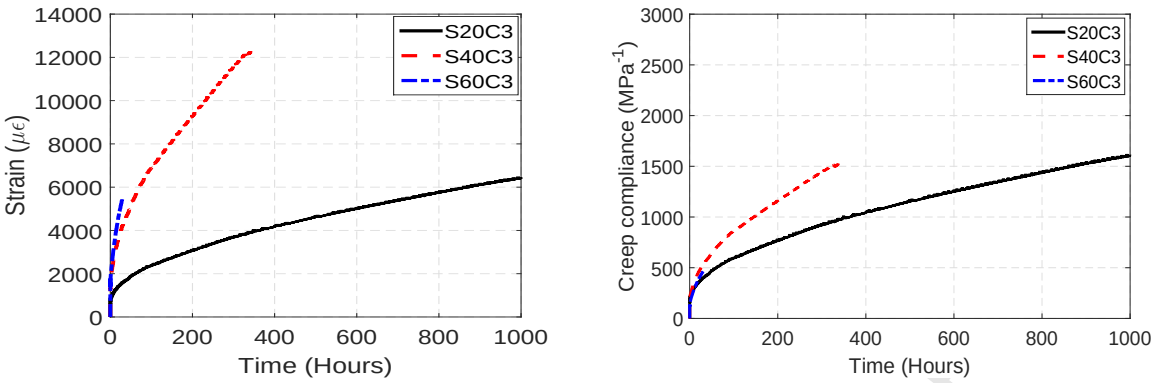

Figure 12: Series 3 (a)Tensile strain with time and (b)Creep compliance with time

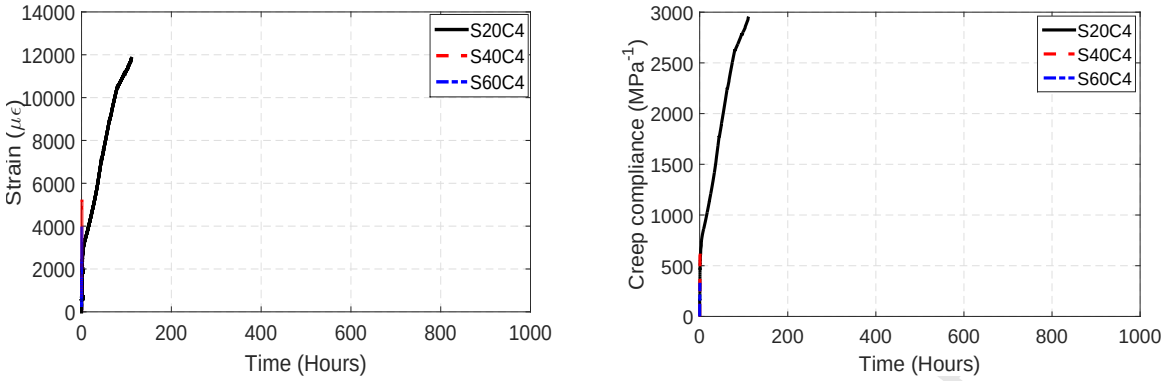

Figure 13: Series 4 (a)Tensile strain with time and (b)Creep compliance with time

List of Tables

Table 1: Tensile creep test matrix.

Series	Specimen ID	Stress level (%)	Temperature °C	Relative humidity (%)
Series 1	S20C1a	20		
	S20C1b	20		
	S40C1a	40	20	55
	S40C1b	40		
	S60C1a	60		
	S60C1b	60		
Series 2	S20C2a	20		
	S20C2b	20		
	S40C2a	40	20	90
	S40C2b	40		
	S60C2a	60		
	S60C2b	60		
Series 3	S20C3a	20		
	S20C3b	20		
	S40C3a	40	40	55
	S40C3b	40		
	S60C3a	60		
	S60C3b	60		
Series 4	S20C4a	20		
	S20C4b	20		
	S40C4a	40	40	90
	S40C4b	40		
	S60C4a	60		
	S60C4b	60		

Table 2: Components determined by SEM.

Element	Weight (%)			
	Object 1	Object 2	Object 3	Object 4
Carbon	13.68	16.21	11.92	72.41
Oxygen	23.35	46.17	42.48	18.67
Sodium	0.26		8.06	
Magnesium			2.08	
Aluminum		0.1	0.41	0.5
Silicon	0.61	37.53	24.47	2.14
Sulfur	11.91		0.13	1.12
Potassium			0.15	
Calcium			7.31	
Barium	50.19			1.46
Chlorine				2.4
Titanium				1.31
Total	100	100	100	100

Table 3: T_g measurements from the different methods (°C)

.

Methodology	DSC			DMA		
	T_{eig}	T_{mg}	T_{efg}	Onset point of storage modulus($E^{'}$)	Loss modulus($E^{''}$)	tan(δ)
T_g (°C)	51.8	52.2	52.5	56.2	60.5	64.3

Table 4: Creep coefficients and creep compliances after 1000 hours.

Series	Specimen ID	Creep coefficient	Creep compliance (1/MPa)	Time to failure (hrs.)
Series 1	S20C1	2.20	375	—
	S40C1	2.26	400	—
	S60C1	3.02	457	—
Series 2	S20C2	2.81	472	—
	S40C2	2.92	496	—
	S60C2	$*$	$*$	60
Series 3	S20C3	10.88	1601	—
	S40C3	$*$	$*$	346
	S60C3	$*$	$*$	30
Series 4	S20C4	$*$	$*$	113
	S40C4	$*$	$*$	1
	S60C4	$*$	$*$	0.5

$*$: Specimen failed